



Overcoming biochar limitations to remediate pentachlorophenol in soil by modifying its electrochemical properties

Francisco J. Chacón^{a,*}, Maria L. Cayuela^a, Harald Cederlund^b, Miguel A. Sánchez-Monedero^a

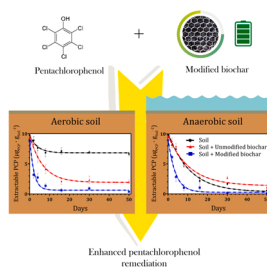
^a Department of Soil and Water Conservation and Organic Waste Management, CEBAS-CSIC, Box 164 Espinardo, 30100 Murcia, Spain

^b Department of Molecular Sciences, Uppsala BioCenter, Swedish University of Agricultural Sciences (SLU), Box 7015, 750 07 Uppsala, Sweden

HIGHLIGHTS

- Raw biochar inhibited PCP remediation in anaerobic soil.
- Biochar modification enhanced PCP remediation in both aerobic and anaerobic soil.
- Biochar redox capacity determines both the rate and extent of PCP remediation.
- Biochar conductivity mainly influences the rate of PCP remediation

GRAPHICAL ABSTRACT



ARTICLE INFO

Keywords:

Designer biochar
Pentachlorophenol
Soil remediation
Redox properties
Conductivity

ABSTRACT

In this study, we produced modified biochars with enhanced electrochemical properties to increase PCP remediation in soil. Although all biochars enhanced PCP remediation in aerobic conditions, only a few did in anaerobic soil. The most successful modifications were (i) the preloading of biomass with 10% w/w FeCl_3 , to obtain a biochar rich in redox-active metals (B-Fe); (ii) the oxidation of a conductive biochar pyrolyzed at 1000 °C with 0.025 M KMnO_4 , to produce a biochar with both moderate conductivity and redox capacity (B-1000- KMnO_4); and (iii) KMnO_4 oxidation of an amorphous biochar pyrolyzed at 400 °C to obtain a biochar with very high redox capacity (B- KMnO_4). B-Fe reduced extractable PCP to almost zero after 50 days in both incubations, but showed slow kinetics of remediation in aerobic soil. B-1000- KMnO_4 had the highest rate of remediation under aerobic conditions, but no significant effect under anaerobic conditions. B- KMnO_4 , however, presented high rates of remediation and high removal of extractable PCP under both conditions, which made it the recommended modification strategy for increased PCP remediation. We found that the degree of remediation primarily depends on the redox capacity, while the rate of remediation was determined by both the conductivity and redox capacity of biochar.

1. Introduction

There is a continuous stream of new chemical and pharmaceutical compounds being produced every year that end up being released into

the environment. Some of them are recalcitrant to degradation, which causes their accumulation and the resulting pollution of soil and water bodies. Among the many novel technologies developed for the remediation of emerging contaminants, biochar is receiving increasing

* Corresponding author.

E-mail address: fjchacon@cebas.csic.es (F.J. Chacón).

<https://doi.org/10.1016/j.jhazmat.2021.127805>

Received 19 September 2021; Received in revised form 11 November 2021; Accepted 12 November 2021

Available online 16 November 2021

0304-3894/© 2021 The Authors.

Published by Elsevier B.V. This is an open access article under the CC BY-NC-ND license

(<http://creativecommons.org/licenses/by-nc-nd/4.0/>).

attention due to its complex and heterogeneous nature (Prado et al., 2019; Rajapaksha et al., 2016; Zheng et al., 2020). One of the contaminants whose degradation is affected by the use of biochar is pentachlorophenol (PCP) (Tong et al., 2014; Zhu et al., 2020), a recalcitrant compound used as an herbicide, pesticide and wood-preserving agent that persists in the environment due to its stable aromatic ring and chlorine content. Its toxicity as a carcinogenic and its neurological and cardiovascular effects causes a serious danger in contaminated soils (Jorens and Schepens, 1993). Besides the immobilization of the contaminant by adsorption (Peng et al., 2016), research has shown that the electrochemical properties of biochar play a key role in the transformation of many pollutants, including PCP (Y. Xu et al., 2019; Yuan et al., 2017). The mechanisms include microbial electron shuttling, direct interspecies electron transfer, Fenton-like processes or the direct redox reaction between biochar and the contaminant, among others (Qian et al., 2018; Wu et al., 2017; X. Xu et al., 2019; Yang et al., 2017; Zhang et al., 2018). In the case of PCP, biochar can serve as an electron transfer mediator, accelerating the electron transfer from cells to PCP, thereby facilitating its degradation through reductive dehalogenation (Yu et al., 2015). However, there have been conflicting results in the remediation of PCP by biochar both in suspension and soil studies. While some articles described an increased degradation of PCP with biochar amendment (Rao et al., 2017; Tong et al., 2014; Zhang et al., 2019), others showed inhibition (Xu et al., 2020; Zhu et al., 2020, 2018). The same has happened with other emerging contaminants, which might be delaying its use in many field applications (Huang et al., 2020; Quilliam et al., 2012). One of the possible sources of the inconsistency in the degradation of PCP is the variability in the electrochemical properties of biochars produced from different sources and pyrolysis methods (Chacón et al., 2020; Klüpfel et al., 2014). A solution to this problem is the modification of biochar to increase its electrochemical properties to an optimal level.

The electrochemical properties of biochar relevant to soil remediation are its conductivity and redox capacity (Chacón et al., 2017). When the temperature of pyrolysis is sufficiently high, condensation of the disordered carbon in biochar creates conductive graphitic sheets able to transfer electrons at very high rates and long distances (Keilueit et al., 2010; Sun et al., 2017). The abundant redox-active functional groups (primarily the quinone/phenolic system), metals and radicals in biochar are considered the major contributors to its redox capacity, which allows biochar to perform both as an electron shuttle and electron buffer (acting as an electron sink or reservoir depending on the redox conditions of soil) (Chacón et al., 2017; Klüpfel et al., 2014). Enhancing the electrochemical properties of biochar requires promoting those components that are responsible for them. Unfortunately, combining both a high redox capacity and a good conductivity is difficult to achieve in unmodified biochars (Chacón et al., 2020, 2017). The highest redox capacities are usually found in biochars produced around a highest treatment temperature (HTT) of 400 °C (Chacón et al., 2017; Klüpfel et al., 2014; PrévotEAU et al., 2016), which is too low for the conductive sheets to develop and form an interconnected network. At temperatures higher than 600 °C, however, thermal degradation removes most of the functional groups responsible for its redox capacity (Harvey et al., 2012). Furthermore, oxidation processes that creates oxygen-containing functional groups in biochar for enhanced redox properties can reduce its conductivity, since these groups preferentially form at the edge of the graphitic sheets, preventing the electron transfer from one sheet to the next (Barton and Koresh, 1984; Polovina et al., 1997). Therefore, modification strategies have to be carefully selected to achieve the desired properties, which must be tailored to the intended application.

In this study, our objective was to examine how modulating the electrochemical properties of biochar can influence PCP remediation in soil and overcome the limitations of the unmodified biochars. We modified biochar through a series of pre- and post-pyrolysis methods tested and characterized in a previous study (Chacón et al., 2020): To produce biochars with high redox capacity (but low conductivity), we

treated a biochar produced at 400 °C with different chemicals to increase its redox-active functionalities. We also preloaded biomass with Fe to create a biochar with a higher concentration of redox metals. In addition, a highly conductive biochar (but with low redox capacity) was produced by increasing pyrolysis HTT to 1000 °C. Lastly, we produced a biochar with both moderate conductivity and redox capacity by treating the biochar pyrolyzed at a HTT of 1000 °C with KMnO₄. We hypothesized that the synergy between conductivity and redox capacity would improve the capacity of biochar to act as an electron shuttle and accelerate the degradation of PCP. Besides the changes caused to the electrochemical properties, biochar modification altered other properties like pH, surface area or the adsorption of the contaminant. Our second objective was to characterize these properties and determine their influence on PCP remediation.

2. Materials and methods

2.1. Chemicals

ABTS (> 98%), iron(III) chloride (FeCl₃, 98%), hydrochloric acid (HCl, 37%), neutral red (> 90%), nitric acid (HNO₃, 70%), pentachlorophenol (97%), potassium hydroxide (KOH, > 85%), potassium permanganate (KMnO₄, > 99%), sodium chloride (NaCl, > 99%), sodium phosphate dibasic (Na₂HPO₄, > 99%) and sodium phosphate monobasic (NaH₂PO₄, > 99%) were obtained from Merck. Hydrogen peroxide (H₂O₂, 30% w/v) and phosphoric acid (H₃PO₄, 88%) were purchased from Panreac. ¹⁴C-PCP (> 95%; approx. 555 MBq·mmol⁻¹) was purchased from IZOTOP, Institute of Isotopes Co., Hungary.

2.2. Biochar production

Olive tree pruning residues were chosen as a renewable feedstock, since woody biochars have been previously found to carry out both conductive and redox-based electron transfer (Chacón et al., 2020; Sun et al., 2017). Previous to pyrolysis, the feedstock was dried, milled and sieved. Slow pyrolysis was performed in a RSR-B 80/500/11 rotatory tube furnace under Ar flux at two highest treatment temperatures (HTT) of 400 °C and 1000 °C. After loading the feedstock, the following heating protocol was applied: (1) from ambient temperature to 105 °C at 5 °C·min⁻¹; (2) 45 min at 105 °C; (3) linear heating to the intended HTT at 5 °C·min⁻¹; (4) 120 min at the HTT (5) cool down. Biochars were grounded by ball milling for 30 s

2.3. Biochar characterization

The characterization of the different biochars was performed in a previous work (Chacón et al., 2020) using the following methods:

C, H, N and S elemental analysis was carried out with a LECO CHNS-932 analyzer. The content of oxygen was calculated by difference (100-C(%)-H(%)-N(%)-Ash(%)). Ash content was determined by heating biochars at 750 °C for 4 h in a muffle furnace.

For the pH measurement, a 1:20 w/v aqueous extract was used following IBI (IBI, 2015). The percentage of neutral form of PCP was calculated with the following equation:

$$\phi_n = \frac{1}{1 + 10^{(pH - pK_a)}} \quad (1)$$

N₂/BET specific surface area was obtained from the N₂ ads/des isotherms obtained in a Micromeritics ASAP 2020 system at 77.4 K.

XPS analysis was carried out in a K-Alpha X-ray system (Thermo Scientific). The instrument is equipped with a monochromated Al K α source (1486.6 eV). Component peak identification was based on previous reported data (Amin et al., 2016).

XRD analysis was performed in a Bruker D8 ADVANCE, where powder samples were scanned over a 10 – 100 °2 θ range.

Metal concentration in biochars were determined using ICP-OES

(ICAP 6500 Duo Thermo) after microwave HNO₃/H₂O₂ digestion.

The conductive properties of biochar were measured with a dielectric spectrometer (Novocontrol GmbH), using a 0.1–107 Hz working range. Sample thickness was 100 μm.

The presence of radicals was measured at room temperature by EPR in a Bruker Elexsys 500.

Biochar electron exchange capacity (EEC, a measure of its redox capacity) was measured with a three-electrode system following Klüpfel et al. (Klüpfel et al., 2014) with some changes. ABTS and neutral red were used as mediators.

2.4. Biochar modification protocols

Modified biochars were produced following the protocols reported in a previous work (Chacón et al., 2020) and were named according to the chemical used for the treatment: Biochar produced at a HTT of 400 °C (B-400) was selected for five post-pyrolysis modifications with H₂O₂, H₃PO₄, HNO₃, KMnO₄ and KOH to obtain a range of biochars with different properties. The KMnO₄ and HNO₃ treatments were used to significantly increase the redox capacity while producing a biochar with a high and low surface area, respectively. The KOH treatment was intended to increase surface area while maintaining the properties of the original biochar. H₃PO₄ modification allowed us to test a biochar with a decreased surface area, redox capacity and graphitic fraction, while the H₂O₂ treatment was selected to oxidize some of the redox-active functional groups on the surface. For the Fe preloaded biochar, 20 g of olive tree pruning biomass and 2 g of FeCl₃ were mixed in 1 L of water, stirred for 24 h, centrifuged, dried overnight and then pyrolyzed at 400 °C. Biochar produced at a HTT of 1000 °C (B-1000) was also treated with KMnO₄ (B-1000-KMnO₄) for a biochar having both moderate conductivity and redox properties.

2.5. Soil sampling and processing

Samples of soil were taken and pooled from the upper layer of a field at Ulleråker (59° 49' N, 17° 39' E), in Sweden. The sieved fraction (Ø < 2 mm) was homogenized and stored until the start of the experiment at 2 °C. Soil moisture was measured by drying the soil for 10 h at 110 °C. WHC was calculated as the moisture left after saturating 30 g of soil with distilled water for 10 h and draining for 4 h. The soil had a pH of 5.9, a composition of 83.7% sand, 8.8% silt and 7.5% clay and a 2.6% of organic matter.

2.6. Adsorption study of PCP on soil-biochar mixtures

Adsorption was determined with the OECD guideline 106 batch equilibrium technique (OECD, 2000). Equilibrium between PCP in solution and adsorbed PCP was reached within 8 h for all cases, as determined in a pre-study. 2 g dry weight of soil and soil-biochar mixtures were added into 50-mL PP tubes and the tubes were filled with 0.01 M CaCl₂ to reach a 1:25 soil/solution ratio. Samples were placed in a shaker at 200 rpm for 8 h under darkness (20 °C). After that, PCP was added to get different concentrations of 2, 5, 10, 20 and 30 μg_{PCP}·g_{soil}⁻¹, with two replicate tubes for each concentration. In addition, 150 μL of ¹⁴C-labelled pentachlorophenol stock solution was added to obtain an activity per sample of 20000 DPM (3.333 × 10⁻⁴ MBq). After 8 h, the samples were centrifuged for 20 min at 3000 rpm. 2 mL of the supernatant and (right before measurement) 4 mL of Quicksafe A scintillation solution were added to scintillation vials. A Beckman LS 6000TA liquid scintillation counter was used to determine ¹⁴C activity, excluding background radioactivity. The distribution coefficient K_d was calculated using the following equation:

$$K_d = \frac{A_{eq}}{100 - A_{eq}} \cdot \frac{V_0}{m_{soil}} \quad (2)$$

where A_{eq} is the equilibrium adsorption percentage; V₀ is the initial volume in the aqueous phase, and m_{soil} represents dry soil mass (g). The distribution coefficient K_d is a useful concept that indicates the relative affinity of PCP to the soil-biochar mixture at equilibrium for a specific concentration. The relationship between K_d and PCP concentration is not linear, so another useful adsorption parameter to obtain is the Freundlich coefficient (K_f) from the adsorption isotherms. The data for the adsorption isotherms were fitted with the Freundlich model in linear form:

$$\log q_e = \log K_f + \frac{1}{n} \log C_e \quad (3)$$

where q_e (μg_{PCP}·g_{soil}⁻¹) is the adsorbed μg of PCP per gram of soil-biochar mixture, C_e (μg_{PCP}·mL⁻¹) is the solution equilibrium concentration, K_f (μg_{PCP}^{1-1/n}·mL^{1/n}·g_{soil}⁻¹) and 1/n are the Freundlich coefficient and the nonlinearity exponent, respectively.

2.7. Soil incubation with PCP

The biochar application rate used in this study of 2.5% g_{biochar}·g_{soil}⁻¹ corresponds to ~33 Mg_{Biochar}·ha⁻¹ assuming a soil bulk density of 1.3 g·cm⁻³ and a soil depth of 10 cm, which was considered optimal for a potential field application. Water content was set following OECD guidelines for aerobic and anaerobic transformations in soil (OECD, 2002). For the PCP concentration, we used Canada as a reference, where the maximum acceptable concentration is 7.6 μg_{PCP}·g_{soil}⁻¹ (CCME, 2007). Different studies (Kitunen et al., 1987; Valo et al., 1984) point to a very variable PCP concentration in contaminated soils, from 0.7 μg_{PCP}·g_{soil}⁻¹ to 45 μg_{PCP}·g_{soil}⁻¹ or even higher in some extreme cases. Therefore, we decided to use an initial PCP concentration of 10 μg_{PCP}·g_{soil}⁻¹. For 10% of each soil sample was spiked with PCP in acetone (acetone only for the control). After being allowed to evaporate for 12 h, the remaining soil was then added and mixed, which resulted in a final PCP concentration of 10 μg_{PCP}·g_{soil}⁻¹. 5 g partitions of soil were placed in plastic tubes and loosely capped for the aerobic incubations, with moisture adjusted to 60% of WHC (maintained for the duration of the experiment). For the anaerobic incubations, 1:2 w/v soil/water mixtures were incubated in glass vials which had the head space purged with N₂ before being sealed. Samples were incubated at 20 °C in the dark. After 2, 4, 8, 16, 32, and 50 days of incubation, three replicates per sample were stored at -20 °C until extraction.

To estimate the kinetics of remediation, the decrease in the concentration of extractable PCP was adjusted to the following exponential decay equation over 50 days, following Li et al. (2019a):

$$C_t = a \cdot e^{-\frac{t}{q}} + b \quad (4)$$

Where C_t is the concentration of PCP at different days, a is the decay intensity constant, t is time in days, q is the decay index and b is a constant. The differential form of the equation can be calculated as follows:

$$\frac{dC_t}{dt} = -\frac{a}{q} \cdot e^{-\frac{t}{q}} = -k_{max} \cdot e^{-\frac{t}{q}} \quad (5)$$

The maximum degradation rate, k_{max} (μg_{PCP}·g_{soil}⁻¹·d⁻¹), is obtained from the values of $\frac{a}{q}$.

2.8. PCP extraction and detection

5 g soil or soil-biochar mixture were extracted with 150 mL of methanol at 250 °C using a Soxtherm system (Gerhardt, Germany). Extraction duration was 180 min. The extracted PCP was determined by HPLC using a Agilent 1260 Infinity system equipped with a C18 column (25 × 0.46 cm) and a diode array detector set at 220 nm. Analyses were performed under isocratic conditions, with a methanol – 1% acetic acid (90/10, v/v) mobile phase. Flow rate was 1 mL·min⁻¹ and the injection

Table 1
Physicochemical characterization of biochars and adsorption coefficients for PCP.

	B-400	B-1000	B-Fe	B-1000-KMnO ₄	B-KMnO ₄	B-HNO ₃	B-H ₃ PO ₄	B-KOH	B-H ₂ O ₂
HTT (°C)	400	1000	400	1000	400	400	400	400	400
EEC (mmol e ⁻ ·g _{Biochar} ⁻¹)	0.413	0.085	0.572	0.418	1.12	0.647	0.366	0.412	0.376
Conductivity (mS·cm ⁻¹)	0.06	3.74	0.02	1.51	0.06	0.05	0.01	0.07	0.01
Radicals (10 ¹¹ spins·g _{Biochar} ⁻¹)	7.54	92.5	1.64	1.65	1.35	1.71	5.71	5.50	3.33
pH (1:20 w/v)	8.97	11.1	7.70	6.06	7.55	3.34	5.09	10.1	7.47
N ₂ -BET Surf. area(m ² ·g _{Biochar} ⁻¹)	11.0	< 2	24.3	14.5	124	2.24	< 2	24.5	4.41
C-OH (at%)	13.8	3.69	12.5	10.1	15.7	16.1	10.7	14.1	11.9
C=O (at%)	3.27	1.87	4.88	3.26	10.2	6.50	2.30	3.01	2.84
COOH (at%)	1.86	2.75	2.67	2.44	2.02	2.67	2.34	1.70	2.93
C-C graphitic (at%)	48.2	64.6	44.9	52.9	46.7	46.2	37.2	43.7	47.4
C-C aliphatic (at%)	12.7	2.70	17.7	7.28	0.97	3.58	26.9	16.8	9.80
S+B mix									
pH (1:2 w/v)	7.62	8.52	6.03	5.68	6.17	4.82	5.29	6.90	5.96
K _d (mL·g _{Soil} ⁻¹)	18.5	13.5	16.2	22.4	42.0	411	33.0	28.8	18.9
K _f (μg _{PCP} ^{1-1/n} ·mL ^{1/n} ·g _{Soil} ⁻¹)	14.5	10.1	12.6	15.8	29.1	244	22.9	20.7	13.9
1/n (nonlinearity exponent)	0.88	0.83	0.93	0.89	0.68	0.92	0.88	0.71	0.92

HTT: Highest treatment temperature of pyrolysis; EEC: Electron exchange capacity; S+B mix: Soil + biochar mixture; K_d: Distribution coefficient for 10 μg_{PCP}·g_{Soil}⁻¹; K_f: Freundlich adsorption coefficient

volume 20 μL. Under these conditions the retention time for pentachlorophenol was 7.35 min

2.9. Treatment of data and statistics

The significance of the differences in the concentration of extractable PCP between soil and soil-biochar mixtures after 50 days of incubation was calculated by one-way analysis of variance (ANOVA), differentiating within groups with Tukey's test ($p < 0.05$). Kendall rank correlation was performed to investigate correlation between the K_d adsorption coefficient and pH values of soil-biochar mixtures. Principal component analysis (PCA) included the following properties and physicochemical parameters of the biochars: electron exchange capacity (EEC), conductivity, abundance of radicals, pH, N₂-BET surface area, Freundlich adsorption coefficient (K_f) and the surface atomic percentages of C-OH, C=O, COOH, graphitic C-C and aliphatic C-C. As component selection method, Kaiser's criterion (only components with eigenvalues of 1.0 or more are selected) was employed. For the principal component regression (PCR), the first-order rate constant k_{max} was selected as the dependent variable.

3. Results and discussion

3.1. Characterization of the modified biochars

The complete characterization of the modified biochars was performed in a previous study (Chacón et al., 2020). Due to the high number of properties (Table 1), principal component analysis (PCA) was

carried out to discover which properties dominated in explaining the variability between biochars. The principal components (PCs) are linear combinations of the different biochar properties that are able to capture most of the variance (information) of the high-dimensional data into a lower dimensional space. In our case, the first three PCs can explain a total of 88.9% of the cumulative variance in the properties of biochars, specifically 47.3% (PC1), 23.5% (PC2) and 18.1% (PC3). The loading values on each PC provide information on how correlated each variable is with that PC and can also be used to visualize the relative correlations between individual variables. Looking at the loadings plot for the PCs that contain more information (Fig. 1A) we can see that most of the variability between biochars is explained by their electrochemical properties (redox capacity measured as EEC and conductivity). As for the relationships between individual variables, properties that contribute to the redox capacity like atomic percentage of C-OH (from electron donating phenolic groups), C=O (electron accepting quinones) or surface area (exposed area for redox reactions to occur) are clustered together near EEC, indicating a positive correlation, while C-C graphitic (aromatic network) is correlated to conductivity. The only exception is the number of radicals, being one of the elements contributing to the redox capacity and yet presenting a negative correlation with EEC. Their destruction during the chemical treatments and their stabilization by resonance in the highly aromatic but low redox B-1000 could explain why radicals are more correlated to conductivity than EEC.

The rest of the properties had minor contributions to variability. Aliphatic C-C was the only variable positively correlated with PC2 with a value higher than 0.5 and was negatively correlated to the rest of the properties due to the inert nature of the group. Adsorption (K_f) and

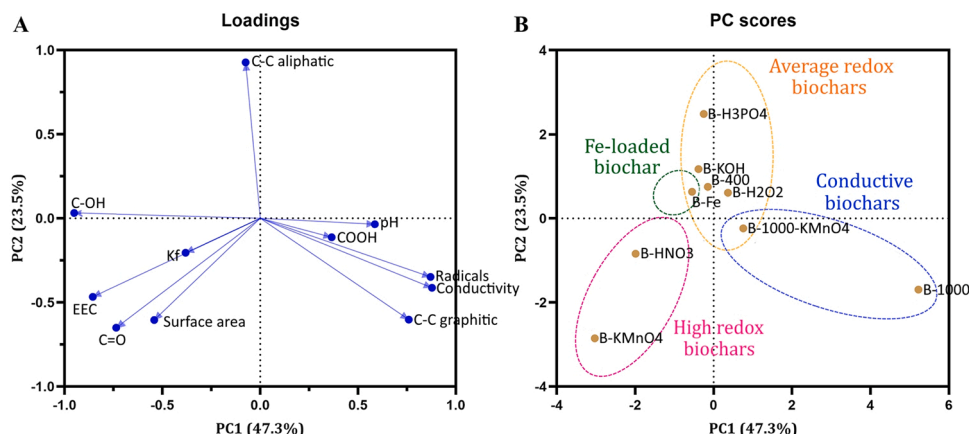


Fig. 1. (A) Loadings and (B) PC scores plot of the first two main components of Principal Component Analysis.

atomic % of COOH had minor contributions to PC1 (< 0.5), while pH was probably related to the high pH of B-1000 and the low pH of the functionalized biochars, except B-KOH. These three properties were the main contributors to PC3, which only explained 18.20% of the variability.

The PC score plot (Fig. 1B) allows us to easily identify the biochar samples that share the properties influencing each PC (closer biochars tend to have similar properties). Therefore, we can divide biochars into three main groups depending on the electrochemical properties they exhibit (Fig. 1B). The bulk of the biochars (B-400, B-H₃PO₄, B-KOH, B-H₂O₂ and B-Fe) had a moderate redox capacity, ranging from the 0.366 mmol e⁻·g_{Biochar}⁻¹ of B-H₃PO₄ to the 0.572 mmol e⁻·g_{Biochar}⁻¹ of the metal preloaded B-Fe (Table 1). Their conductivity was almost non-existent, coming from an original biochar produced at a too low HTT (400 °C) to form a conductive network. In addition, the treatments further disrupted the aromatic structure as seen by the reduction in the atomic percentage of C-C graphitic groups and conductivity. B-KMnO₄ and B-HNO₃ had the highest electron exchange capacities of all biochars, especially B-KMnO₄ (1.115 mmol e⁻·g_{Biochar}⁻¹). The increased redox capacity came mainly from a higher amount of phenolic (C-OH) and quinone groups (C=O), since the washing steps of the treatment removed most of the redox-active Mn from its surface (Table S1). They were also able to maintain most the graphitic structure on the surface while removing the aliphatic fraction (probably by functionalization). H₃PO₄ treatment, on the other hand, besides not being capable of introducing new redox-active groups, also severely affected the integrity of the graphite-like fraction. This, combined with the low surface area resulted in a biochar with lower redox capacity than the original and a higher fraction of aliphatic C-C. B-1000 and B-1000-KMnO₄ were the only biochars with considerable conductivity, thanks to the HTT of 1000 °C at which they were pyrolyzed, which produced biochars with an extensive aromatic structure. As indicated in the introduction, the addition of oxygen-containing functional groups by the KMnO₄ treatment lowered the conductivity of the B-1000-KMnO₄ biochar, since they are preferentially introduced at the edges of the graphite sheets, hampering the electron transfer between them. Still, it retained a conductivity that was more than 20 times higher than the rest of biochars, while obtaining an average redox capacity.

3.2. Adsorption of PCP

According to the values of the Freundlich adsorption constant (K_f) and the distribution coefficient (K_d) for soil-biochar mixtures (Table 1, Fig. S1), the adsorption capacity compared to soil (K_f = 14 μg_{PCP}^{1-1/n}·mL^{1/n}·g_{soil}⁻¹ and K_d = 20 mL·g_{soil}⁻¹) was significantly higher in all treated biochars except B-Fe, while the lowest adsorption was found in B-1000. One of the main drivers of PCP adsorption to biochar is pH (Peng et al., 2016). At a low pH (especially below its pK_a of 4.7) the neutral form of PCP will favor adsorption via π-π interactions with the aromatic network of the biochar. As expected, the Kendall rank correlation test between the K_d adsorption coefficients and pH values of soil-biochar mixtures showed a significant negative correlation (r_τ = -0.556, p < 0.05). The highly redox-active and functionalized biochars had a lower pH than the rest, which could explain the close clustering and therefore positively correlation of the K_f and EEC loadings. B-HNO₃ had the lowest pH (4.82) of all biochars and its soil-biochar mixture presented a pH close to the pK_a of PCP. Consequently, 43% of PCP was in neutral form and its adsorption was one order of magnitude higher than the rest. B-H₃PO₄ had also a pH close to 5, in this case with 20% of PCP in neutral form. This resulted in a high adsorption, even when the proportion of graphitic C-C in the surface remained low. The rest of soil-biochar mixtures had less than 10% of PCP in neutral form and their adsorption probably depended on other properties like surface area and graphitic C-C.

The Freundlich model of adsorption assumes a heterogeneous surface (which is the common case in biochar), where a lower value of the

1/n exponent can be linked to a higher degree of binding site heterogeneity of the material (Salame and Bandosz, 2003; Tseng and Wu, 2008). This heterogeneity arises from the presence of different quantities and types of functional groups, bound impurities, and a heterogeneous pore structure distribution on the surface. In our study, most treatments decreased the heterogeneity of the biochar compared to the untreated biochars, as seen by their higher 1/n value (Table 1). Despite the introduction of new functionalities and heteroatoms, the collapse of many of the pores on the surface probably reduced the structural heterogeneity of biochar, as can be seen by the lower pore volume and pore surface area in most of the treated samples (Table S2). B-KMnO₄ and B-KOH (the two biochars with the highest surface areas) were the exception having a higher heterogeneity than the original biochars. They showed increased pore surface area and average pore volume, which suggests the formation of new pores. Although B-1000-KMnO₄ was subjected to the same treatment as B-KMnO₄, its heterogeneity was much lower. This is probably due to the more stable and resistant aromatic network produced after pyrolyzing at 1000 °C compared to the amorphous carbon structure of the 400 °C pyrolysis, which prevented the formation of pores and the introduction of more functional groups.

Thanks to the relationship between soil/solution ratios and the distribution coefficient K_d (Fig. S2), we can estimate the amount of PCP adsorbed to soil-biochar mixtures (OECD, 2000), which was > 90% in all aerobic incubations and > 80% in anaerobic ones.

3.3. Remediation of PCP

The average recoveries of PCP at 8 h of incubation ranged from 85.8% to 98.4% (Table S3), showing the suitability of the extraction method to recover the adsorbed contaminant. Besides the loss of PCP due to mineralization and incorporation to microbial structures, its irreversible bonding and complexation to soil organic matter makes it difficult to extract all of the contaminant present in soil. Despite this, soil-bound contaminants, including PCP, can be considered detoxified since they have a very low bioavailability, the complexed products are less toxic and leaching of the chemical is restricted (Banks and Schwab, 2006; Bollag, 2002; Spagnuolo et al., 2010). Furthermore, a strong extraction capable of recovering the bound fraction could result in overestimating its bioavailability and real toxicity in soil (Kelsey and Alexander, 1997). Therefore, we considered extractable PCP as a good proxy for the bioavailable PCP in soil.

The amount of extractable PCP recovered from soils after 50 days of incubation is presented in Fig. 2A and B. In the aerobic incubations, all biochars were able to decrease the concentration of PCP compared to soil without biochar. Unamended soil showed a mere 33.6% reduction in extractable PCP, while even the least effective biochar amendment (B-H₃PO₄) was able to remove an average 71.2% of the contaminant. PCP can be very recalcitrant to degrade in aerated soils, especially if they have a low organic matter content like was our case (Rao, 1978). B-KMnO₄ (the biochar with the highest redox capacity), B-Fe (with redox-active metal) and B-1000-KMnO₄ (balanced with moderate conductivity and redox capacity) were the most successful biochars, being able to remove almost all extractable PCP from soil, which proved that different strategies can be used to enhance PCP remediation in aerobic soils. This is important, since the minimum concentration at which PCP exhibits toxicity can be as low as 0.01 μg·g_{soil}⁻¹ (Martí et al., 2007). Also, the fact that there is a high plateau in the unamended soil shows that we were able to overcome not only the limitations of biochar to but also of the soil itself.

In the anaerobic incubations, however, our results align with those that reported inhibition in the degradation of PCP after biochar addition. Unlike in the aerobic situation, after 50 days unamended anaerobic soil was very successful at reducing the concentration of PCP, having only an average of 5.5% of the initial spiked contaminant. From our nine biochar amendments, four significantly inhibited PCP remediation (including the unmodified biochars, B-400 and B-1000) and three showed no

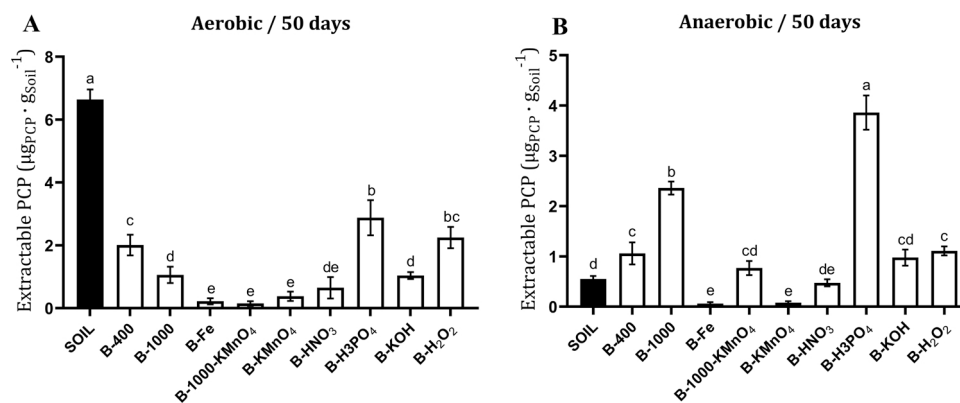


Fig. 2. Extractable PCP after 50 days of (A) aerobic and (B) anaerobic incubations of soil and soil-biochar mixtures. The initial spiked concentration was $10 \mu\text{g}_{\text{PCP}} \cdot \text{g}_{\text{Soil}}^{-1}$. Error bars represent \pm SD ($n = 3$). Letters upon bars indicate significant differences ($p < 0.05$).

significant difference with the unamended soil. Only B-Fe and B-KMnO₄ were able to overcome the limitations of the unmodified biochar, reducing PCP levels to almost zero. Contrary to our expectations, the biochar with balanced electrochemical properties (B-1000-KMnO₄) was not able to improve remediation compared to unamended soil, perhaps due to an insufficient number of redox-active groups. Still, extractable PCP was reduced to only 7.7% of the initial spiked concentration. B-H₃PO₄ and B-1000 were the worst biochar amendments in anaerobic soil, with a concentration of extractable PCP several times that of unamended soil. These were the two biochars with the lowest redox capacities, which indicates a key role of this property in the remediation of PCP in anaerobic soils.

3.4. Kinetics of PCP remediation

The rate at which the remediation occurs can be as important as the eventual complete removal of PCP from soil. Remediation is mostly employed in situations where the inherent rate of degradation is very slow and speeding up the process is an important practical and economic consideration. Since biochar is thought to facilitate electron transfer from cells to PCP during biodegradation, modified biochars with higher redox properties and conductivities are expected to show increased kinetics of remediation. The evolution in the concentration of extractable PCP at different days is presented in Fig. 3 A-D. As expected, B-1000-KMnO₄ (balanced biochar with moderate conductivity and redox capacity) and B-KMnO₄ (highest redox capacity) had the highest maximum rates of remediation (k_{max}) in both incubations (Table 2). In the aerobic incubation, the extractable concentration of PCP in unamended soil was only

reduced by 33.6%, while in just 4 days B-1000-KMnO₄ remediated 84.3% of spiked PCP and B-KMnO₄ was able to remove 80.6% in 8 days. As for the anaerobic incubation, even though most of the contaminant disappeared from unamended soil, in only 16 days B-KMnO₄, B-1000-KMnO₄ and B-Fe reduced extractable PCP to levels not seen in the unamended soil until after 50 days of incubation. Even though the rates of remediation were generally slower under anaerobic conditions compared to the aerobic soil, their relationship to the electron exchange capacity of the biochars was similar (Fig. 3E and F). There was a significant linear correlation between EEC and k_{max} for all biochars with low conductivity, except B-Fe. The conductive biochars, however, had much higher remediation rates than one would expect from their EEC alone. The concentration of extractable PCP after 50 days for the B-1000 amendment was higher than in other biochar amendments (in both incubations) and B-1000-KMnO₄ was not able to enhance remediation in the anaerobic soil (especially compared to biochars with higher EEC, which did improve remediation). This suggests that the main contribution of conductivity is in the rate of remediation, while the redox capacity has a role in both the rate and the extent of PCP remediation.

Although B-Fe almost completely removed extractable PCP after 50 days in both incubations, its k_{max} was very low in the aerobic soil (Fig. 3C, Table 2). Previous studies have demonstrated that Fe(II) is able to react with halogenated contaminants, including pentachlorophenol, to cause their reductive dehalogenation (Li et al., 2008; Maithreepala and Doong, 2009). Furthermore, PCP reduction rates correlate with soil Fe availability (Chen et al., 2014). B-Fe presents magnetite on its surface (Fig. S3), a mineral that contains both Fe(II) and Fe(III). In the presence of oxygen, however, Fe(II) tends to be oxidized to Fe(III), which could compete with PCP as a terminal electron acceptor (Zhu et al., 2020, 2018), reducing the rate of microbial dehalogenation. This could explain the slow kinetics of remediation for the aerobic soil. In the absence of oxygen, however, the formation of Fe(II) is favored again (Colombo et al., 2013). It has been reported that biochar can also donate electrons to Fe(III) to form Fe(II), especially in the presence of microorganisms, which can accelerate the process (Xu et al., 2016; Zhou et al., 2017). This resulted in a much higher maximum remediation rate in the anaerobic soil (Fig. 3D, Table 2).

To help in identifying the influence of the rest of the properties in the kinetics of remediation, principal components regression (PCR, a combination of multiple linear regression and principal component analysis.) was performed with k_{max} as the dependent variable. Using all biochars in the analysis, not a single property had a significant impact on the outcome of k_{max} (Table S4). However, PCR is sensitive to outliers, whose presence can lead to a bad interpretation of the results (Serneels and Verdonck, 2009). From Fig. 3E and F, we can select B-1000-KMnO₄ as a probable candidate for an outlier, perhaps due to the synergy between conductivity and redox capacity. After repeating the analysis for the aerobic incubation, the model ($R^2 = 0.902$, $p < 0.05$) showed that EEC, surface area, C=O, C-OH, and graphitic C-C had a significant positive impact on k_{max} , while aliphatic C-C had a negative impact. The same results were found for the anaerobic incubation ($R^2 = 0.891$, $p < 0.05$), except graphitic C-C, which was non-significant. This suggests that the only properties that contribute to the rate of remediation are those that are directly or indirectly (surface area) related to the electrochemical properties. One possible shortcoming is that PCA reduces dimensionality by creating linear combinations of the original variables. As a consequence, nonlinear relationships between k_{max} and the different variables cannot be identified, which may be the case for some properties like conductivity or pH.

3.5. Possible influence of biochar on PCP transformation pathways

Microbial dehalogenation is thought to be the main pathway of PCP transformation in soil, although some oxidative degradation is also found, especially in an aerobic environment (D'Angelo and Reddy, 2000; Rao, 1978). Biochar can amplify this reductive process by acting as an electron donor to the halo-respiring bacteria that use PCP as

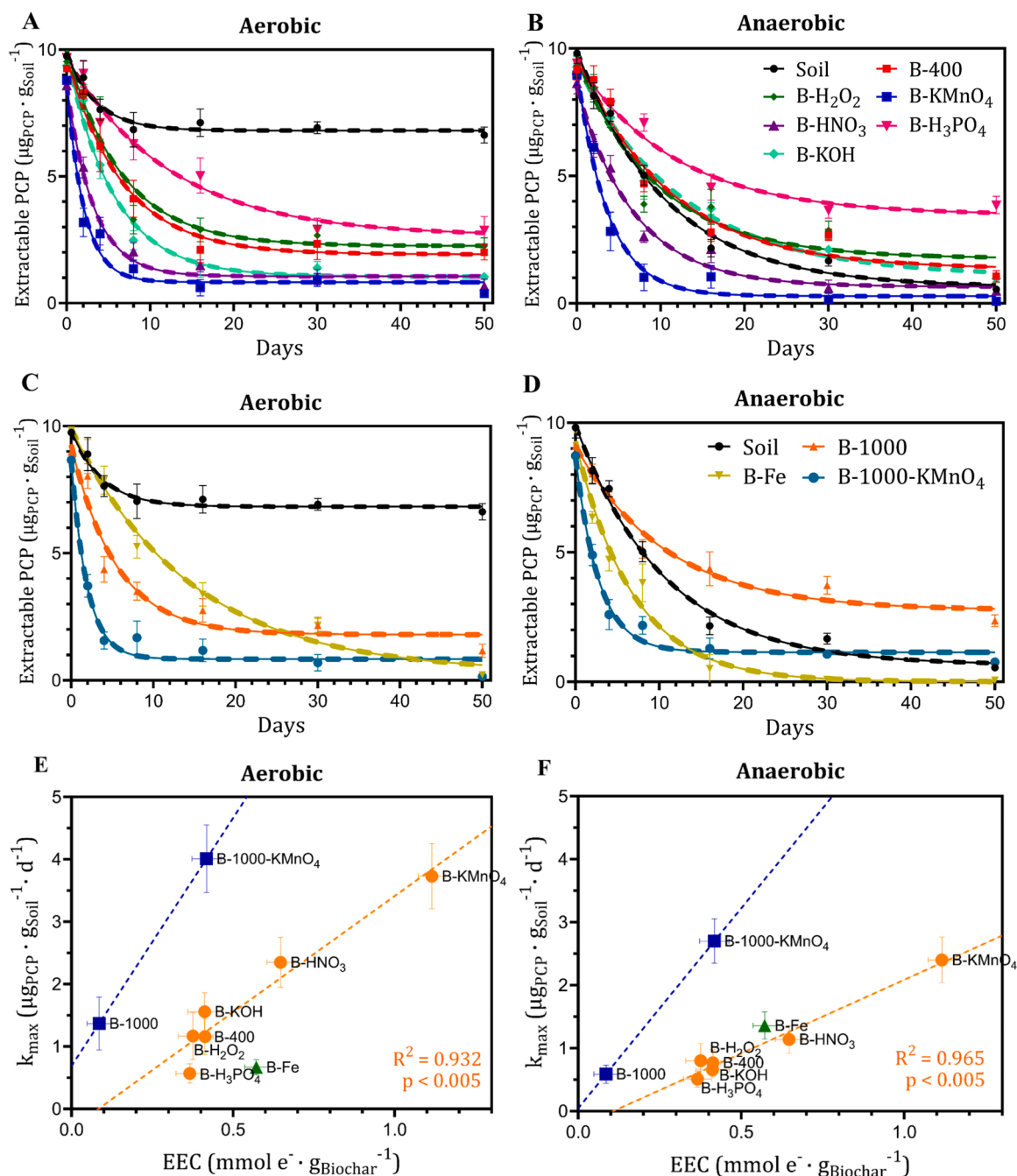


Fig. 3. Evolution in the concentration of extractable PCP in (A, C) aerobic and (B, D) anaerobic incubations, with lines showing the results of the fitted exponential decay Eq. (4). The relationship between remediation rate k_{max} and EEC in (E) aerobic and (F) anaerobic incubations is also shown. Colors grouped conductive (blue), functionalized (orange) and Fe-loaded biochars (green). Error bars represent \pm SD ($n = 3$).

terminal electron acceptor (Yu et al., 2015). This would increase both the rate and extent of PCP remediation, as we see in the biochar amendments with the highest redox capacities (B- KMnO_4 and B- HNO_3). In the case of the conductive biochars, the presence of a developed graphitic structure results in long-range electron transfer. This allows for a multitude of beneficial mechanisms to the electron shuttle activity, such as the transfer of electrons from electron-rich to electron-depleted areas in biochar, the coupling of different microbial metabolisms or the regeneration of oxidized functional groups. Additionally, the abundance of functional groups in the conductive B-1000- KMnO_4 biochar can facilitate this electron transfer by adsorbing cells to the surface. Microbial cytochromes are known to attach to surface oxygen-containing functional groups, which might increase the electron transfer between

biochar, cells and the adsorbed PCP (Li and Cheng, 2019; Li et al., 2019b; Wang et al., 2018). Conductivity would mostly accelerate PCP reduction, as the amount of transformed PCP would still depend in the end on the reductive potential of the soil, the microbial population and the electron donating capacity of biochar.

The high adsorption of PCP by all biochars could potentially immobilize the contaminant, preventing the contact of PCP with microorganisms and therefore its reduction. Indeed, despite its role as an electron mediator, biochar amendment can inhibit the biodegradation of some contaminants due to a decreased bioavailability (Loganathan et al., 2009; Ukalska-Jaruga et al., 2019). However, in our case three of the four biochars with the highest adsorption (B- KMnO_4 , B- HNO_3 and B-Fe) were among the amendments with the highest remediation levels.

Table 2
Kinetics of PCP remediation and % of PCP removal after 50 days.

	Aerobic			Anaerobic		
	k_{\max} ($\mu\text{g}_{\text{PCP}} \cdot \text{g}_{\text{soil}}^{-1} \cdot \text{d}^{-1}$)	R^2	% PCP removal (50 d)	k_{\max} ($\mu\text{g}_{\text{PCP}} \cdot \text{g}_{\text{soil}}^{-1} \cdot \text{d}^{-1}$)	R^2	% PCP removal (50 d)
Soil	0.81	0.837	33.6	0.88	0.983	94.5
B-400	1.16	0.956	79.9	0.77	0.950	89.4
B-1000	1.37	0.931	89.3	0.59	0.956	76.4
B-Fe	0.67	0.977	97.8	1.36	0.970	99.4
B-1000-KMnO ₄	4.01	0.964	98.5	2.70	0.976	92.3
B-KMnO ₄	3.73	0.960	96.2	2.40	0.969	99.2
B-HNO ₃	2.35	0.976	93.5	1.14	0.971	95.3
B-H ₃ PO ₄	0.57	0.950	71.2	0.51	0.959	61.4
B-KOH	1.56	0.971	89.6	0.66	0.975	90.2
B-H ₂ O ₂	1.17	0.928	77.5	0.80	0.926	88.9

The exception, B-H₃PO₄, had no conductivity, was the biochar with the lowest redox capacity and had among the lowest atomic percentages of C-OH and C=O functional groups. This supports the hypothesis that PCP can be abiotically reduced on the surface of biochar, probably by its interaction with the aromatic network, electron donating phenolic groups, radicals and redox-active metals on the surface of biochar (Li et al., 2008; Yu et al., 2015). Thus, adsorption would increase PCP remediation for those modified biochars with a high redox capacity and/or redox metals, while it would be detrimental to those with low or moderate redox capacities, especially in conditions of low soil reductive potential. Conductivity could overcome this problem to some extent by transferring electrons from one part of biochar to another, which may explain the higher and faster remediation of the B-1000-KMnO₄ biochar compared to B-400 in aerobic soil, even though they have similar redox capacities.

In the aerobic incubation, conditions are not ideal for PCP transformation. Therefore, the contribution of biochar electrochemical properties both in mediation and direct electron donation was probably enough to enhance remediation in all biochar amendments. Under the right conditions, such as high soil reductive potential, PCP degradation can be significant, as seen in the unamended anaerobic incubation. This led to inhibition for biochars with a low amount of redox-active functionalities or metals in the anaerobic incubation (such as B-400, B-1000, B-H₂O₂ and especially B-H₃PO₄). To increase remediation in these conditions, a very large amount of redox-active moieties would need to be present. This was precisely the case with B-KMnO₄ and B-Fe, the only biochar amendments that significantly increased PCP remediation in anaerobic soil. B-KMnO₄ showed the highest redox capacity and surface area of all biochars, while B-Fe was the only one with a high amount of redox-active metal.

4. Conclusions

In this study we were able to modify the electrochemical properties of biochar to enhance the remediation of pentachlorophenol in soil. Multivariate analysis of biochar properties indicated that only its electrochemical properties and surface area were relevant contributors to the rate of remediation. B-KMnO₄, B-Fe and B-1000-KMnO₄ were the most successful biochars amendments in our study. Although B-1000-KMnO₄ had the highest kinetics of remediation of all biochars, there was no significant difference with unamended soil in the anaerobic incubation. B-Fe was able to almost completely remediate soil in both types of incubation, but its slow kinetics in the aereated soil could result in toxicity and bioaccumulation. Therefore, considering both aerobic and anaerobic situations, we propose that the best modification to enhance PCP remediation is to increase the redox capacity of biochar by KMnO₄ treatment. This demonstrates the feasibility of producing designer biochars with optimal electrochemical properties for specific applications. For example, for contaminants that can be chemically transformed on the surface of biochar the ideal properties are a very high redox capacity and surface area, which can be obtained treating a biochar pyrolyzed at

an intermediate HTT with KMnO₄. If biodegradation is the main driver and a long-term effect of biochar application is desired, KMnO₄ treatment to a conductive biochar obtained at 1000 °C will result in a biochar with an outstanding electron shuttle ability and high resistance to oxidation thanks to its stable graphitic structure. In the same way, applications that require other properties like a certain pH or the presence of redox-active metals can be satisfied by selecting the appropriate treatment.

CRedit authorship contribution statement

Francisco J. Chacón: Conceptualization, Methodology, Formal analysis, Investigation, Writing – original draft & review, Visualization. **Maria L. Cayuela:** Conceptualization, Methodology, Validation, Resources, Writing – review & editing, Supervision. **Harald Cederlund:** Conceptualization, Methodology, Validation, Resources, Writing – review & editing, Supervision. **Miguel A. Sánchez-Monedero:** Conceptualization, Methodology, Validation, Resources, Writing – review & editing, Supervision.

Declaration of Competing Interest

The authors declare that they have no known competing financial interests or personal relationships that could have appeared to influence the work reported in this paper.

Acknowledgments

Financial support of projects N° CTM2015–67200-R and RTI2018-099417-B-I00, financed by the Spanish Ministry of Economy and Competitiveness and the Spanish Ministry of Science, Innovation and Universities, cofunded with EU FEDER funds, is greatly appreciated.

Appendix A. Supporting information

Supplementary data associated with this article can be found in the online version at [doi:10.1016/j.jhazmat.2021.127805](https://doi.org/10.1016/j.jhazmat.2021.127805).

References

- Amin, F.R., Huang, Y., He, Y., Zhang, R., Liu, G., Chen, C., 2016. Biochar applications and modern techniques for characterization. *Clean. Technol. Environ. Policy* 18, 1457–1473. <https://doi.org/10.1007/s10098-016-1218-8>.
- Banks, M.K., Schwab, A.P., 2006. Ecotoxicity of Pentachlorophenol in Contaminated Soil as Affected by Soil Type. *J. Environ. Sci. Health, Part A* 41, 117–128. <https://doi.org/10.1080/10934520500348559>.
- Barton, S.S., Koresh, J.E., 1984. A study of the surface oxides on carbon cloth by electrical conductivity. *Carbon* 22, 481–485. [https://doi.org/10.1016/0008-6223\(84\)90079-4](https://doi.org/10.1016/0008-6223(84)90079-4).
- Bollag, J.M., 2002. *Immobilisation of pesticides in soil through enzymatic reactions. In: Biotechnology for the Environment*. Springer.
- CCME, 2007. Interim Canadian environmental quality criteria for contaminated sites. Canadian Council of Ministers of the Environment, Winnipeg, Canada. <https://>

- www.esdat.net/environmental%20standards/canada/soil/rev_soil_summary_tbl_7_0_e.pdf.
- Chacón, F.J., Cayuela, M.L., Roig, A., Sánchez-Monedero, M.A., 2017. Understanding, measuring and tuning the electrochemical properties of biochar for environmental applications. *Rev. Environ. Sci. Bio/Technol.* 16, 695–715. <https://doi.org/10.1007/s11157-017-9450-1>.
- Chacón, F.J., Sánchez-Monedero, M.A., Lezama, L., Cayuela, M.L., 2020. Enhancing biochar redox properties through feedstock selection, metal preloading and post-pyrolysis treatments. *Chem. Eng. J.* 395, 125100. <https://doi.org/10.1016/j.cej.2020.125100>.
- Chen, M., Tao, L., Li, F., Lan, Q., 2014. Reductions of Fe(III) and pentachlorophenol linked with geochemical properties of soils from Pearl River Delta. *Geoderma* 217–218, 201–211. <https://doi.org/10.1016/j.geoderma.2013.12.003>.
- Colombo, C., Palumbo, G., He, J.-Z., Pinton, R., Cesco, S., 2013. Review on iron availability in soil: interaction of Fe minerals, plants, and microbes. *J. Soils Sediment.* 14, 538–548. <https://doi.org/10.1007/s11368-013-0814-z>.
- D'Angelo, E.M., Reddy, K.R., 2000. Aerobic and Anaerobic Transformations of Pentachlorophenol in Wetland Soils. *Soil Sci. Soc. Am. J.* 64, 933–943. <https://doi.org/10.2136/sssaj2000.643933x>.
- Harvey, O.R., Herbert, B.E., Kuo, L.-J., Louchouart, P., 2012. Generalized Two-Dimensional Perturbation Correlation Infrared Spectroscopy Reveals Mechanisms for the Development of Surface Charge and Recalcitrance in Plant-Derived Biochars. *Environ. Sci. Technol.* 46, 10641–10650. <https://doi.org/10.1021/es302971d>.
- Huang, T., Ding, T., Liu, D., Li, J., 2020. Degradation of Carbendazim in Soil: Effect of Sewage Sludge-Derived Biochars. *J. Agric. Food Chem.* 68, 3703–3710. <https://doi.org/10.1021/acs.jafc.9b07244>.
- IBI, 2015. Standardized product definition and product testing guidelines for biochar that is used in soil. Version 2.1.
- Jorens, P.G., Schepens, P.J.C., 1993. Human Pentachlorophenol Poisoning. *Hum. Exp. Toxicol.* 12, 479–495. <https://doi.org/10.1177/096032719301200605>.
- Keilueit, M., Nico, P.S., Johnson, M.G., Kleber, M., 2010. Dynamic Molecular Structure of Plant Biomass-Derived Black Carbon (Biochar). *Environ. Sci. Technol.* 44, 1247–1253. <https://doi.org/10.1021/es9031419>.
- Kelsey, J.W., Alexander, M., 1997. Declining bioavailability and inappropriate estimation of risk of persistent compounds. *Environ. Toxicol. Chem.* 16, 582–585. <https://doi.org/10.1002/etc.5620160327>.
- Kitunen, V.H., Valo, R.J., Salkinoja-Salonen, M.S., 1987. Contamination of soil around wood-preserving facilities by polychlorinated aromatic compounds. *Environ. Sci. Technol.* 21, 96–101. <https://doi.org/10.1021/es00155a012>.
- Klüpfel, L., Keilueit, M., Kleber, M., Sander, M., 2014. Redox Properties of Plant Biomass-Derived Black Carbon (Biochar). *Environ. Sci. Technol.* 48, 5601–5611. <https://doi.org/10.1021/es500906d>.
- Li, C., Cheng, S., 2019. Functional group surface modifications for enhancing the formation and performance of exoelectrogenic biofilms on the anode of a bioelectrochemical system. *Crit. Rev. Biotechnol.* 39, 1015–1030. <https://doi.org/10.1080/07388551.2019.1662367>.
- Li, F., Wang, X., Liu, C., Li, Y., Zeng, F., Liu, L., 2008. Reductive transformation of pentachlorophenol on the interface of suboptimal soil colloids and water. *Geoderma* 148, 70–78. <https://doi.org/10.1016/j.geoderma.2008.09.003>.
- Li, H., Chen, S., Ren, L.Y., Zhou, L.Y., Tan, X.J., Zhu, Y., Belver, C., Bedia, J., Yang, J., 2019a. Biochar mediates activation of aged nanoscale ZVI by Shewanella putrefaciens CN32 to enhance the degradation of Pentachlorophenol. *Chem. Eng. J.* 368, 148–156. <https://doi.org/10.1016/j.cej.2019.02.099>.
- Li, H., Wang, B., Deng, S., Dai, J., Shao, S., 2019b. Oxygen-containing functional groups on bioelectrode surface enhance expression of c-type cytochromes in biofilm and boost extracellular electron transfer. *Bioresour. Technol.* 292, 121995. <https://doi.org/10.1016/j.biortech.2019.121995>.
- Loganathan, V.A., Feng, Y., Sheng, G.D., Clement, T.P., 2009. Crop-Residue-Derived Char Influences Sorption, Desorption and Bioavailability of Atrazine in Soils. *Soil Sci. Soc. Am. J.* 73, 967–974. <https://doi.org/10.2136/sssaj2008.0208>.
- Maithreepala, R.A., Doong, R., 2009. Transformation of carbon tetrachloride by biogenic iron species in the presence of Geobacter sulfurreducens and electron shuttles. *J. Hazard. Mater.* 164, 337–344. <https://doi.org/10.1016/j.jhazmat.2008.08.007>.
- Martí, E., Sierra, J., Sánchez, M., Cruañas, R., Garau, M.A., 2007. Ecotoxicological tests assessment of soils polluted by chromium (VI) or pentachlorophenol. *Sci. Total Environ.* 378, 53–57. <https://doi.org/10.1016/j.scitotenv.2007.01.012>.
- OECD, 2000. Adsorption/desorption using a batch equilibrium method. OECD Test Guideline 106, Paris, France. <https://doi.org/10.1787/20745753>.
- OECD, 2002. Aerobic and Anaerobic Transformation in Soil. OECD Guidelines for Testing of Chemicals, Section 3, Test No 307, Paris, France. <https://doi.org/10.1787/2074577x>.
- Peng, P., Lang, Y.-H., Wang, X.-M., 2016. Adsorption behavior and mechanism of pentachlorophenol on reed biochars: pH effect, pyrolysis temperature, hydrochloric acid treatment and isotherms. *Ecol. Eng.* 90, 225–233. <https://doi.org/10.1016/j.ecoleng.2016.01.039>.
- Polovina, M., Babić, B., Kaluderović, B., Dekanski, A., 1997. Surface characterization of oxidized activated carbon cloth. *Carbon* 35, 1047–1052. [https://doi.org/10.1016/s0008-6223\(97\)00057-2](https://doi.org/10.1016/s0008-6223(97)00057-2).
- Prado, A., Berenguer, R., Esteve-Núñez, A., 2019. Electroactive biochar outperforms highly conductive carbon materials for biodegrading pollutants by enhancing microbial extracellular electron transfer. *Carbon* 146, 597–609. <https://doi.org/10.1016/j.carbon.2019.02.038>.
- PrévotEAU, A., Ronsse, F., Cid, I., Boeckx, P., Rabaey, K., 2016. The electron donating capacity of biochar is dramatically underestimated. *Sci. Rep.* 6. <https://doi.org/10.1038/srep32870>.
- Qian, X., Ren, M., Fang, M., Kan, M., Yue, D., Bian, Z., Li, H., Jia, J., Zhao, Y., 2018. Hydrophilic mesoporous carbon as iron(III)/(II) electron shuttle for visible light enhanced Fenton-like degradation of organic pollutants. *Appl. Catal. B: Environ.* 231, 108–114. <https://doi.org/10.1016/j.apcatb.2018.03.016>.
- Quilliam, R.S., Rangecroft, S., Emmett, B.A., Deluca, T.H., Jones, D.L., 2012. Is biochar a source or sink for polycyclic aromatic hydrocarbon (PAH) compounds in agricultural soils? *GCB Bioenergy* 5, 96–103. <https://doi.org/10.1111/gcbb.12007>.
- Rajapaksha, A.U., Chen, S.S., Tsang, D.C.W., Zhang, M., Vithanage, M., Mandal, S., Gao, B., Bolan, N.S., Ok, Y.S., 2016. Engineered/designer biochar for contaminant removal/immobilization from soil and water: Potential and implication of biochar modification. *Chemosphere* 148, 276–291. <https://doi.org/10.1016/j.chemosphere.2016.01.043>.
- Rao, K., 1978. Pentachlorophenol: Chemistry, Pharmacology, and Environmental Toxicology. Springer. <https://doi.org/10.1007/978-1-4615-8948-8>.
- Rao, M.A., Di Rauso Simeone, G., Scelza, R., Conte, P., 2017. Biochar based remediation of water and soil contaminated by phenanthrene and pentachlorophenol. *Chemosphere* 186, 193–201. <https://doi.org/10.1016/j.chemosphere.2017.07.125>.
- Salame, I.L., Bandoz, T.J., 2003. Role of surface chemistry in adsorption of phenol on activated carbons. *J. Colloid Interface Sci.* 264, 307–312. [https://doi.org/10.1016/s0021-9797\(03\)00420-x](https://doi.org/10.1016/s0021-9797(03)00420-x).
- Serneels, S., Verdonck, T., 2009. Principal component regression for data containing outliers and missing elements. *Comput. Stat. Data Anal.* 53, 3855–3863. <https://doi.org/10.1016/j.csda.2009.04.008>.
- Spagnuolo, M., Puglisi, E., Vernile, P., Bari, G., de Lillo, E., Trevisan, M., Ruggiero, P., 2010. Soil monitoring of pentachlorophenol by bioavailability and ecotoxicity measurements. *J. Environ. Monit.* 12, 1575. <https://doi.org/10.1039/b925026c>.
- Sun, T., Levin, B.D.A., Guzman, J.J.L., Enders, A., Muller, D.A., Angenent, L.T., Lehmann, J., 2017. Rapid electron transfer by the carbon matrix in natural pyrogenic carbon. *Nat. Commun.* 8. <https://doi.org/10.1038/ncomms14873>.
- Tong, H., Hu, M., Li, F.B., Liu, C.S., Chen, M.J., 2014. Biochar enhances the microbial and chemical transformation of pentachlorophenol in paddy soil. *Soil Biol. Biochem.* 70, 142–150. <https://doi.org/10.1016/j.soilbio.2013.12.012>.
- Tseng, R.-L., Wu, F.-C., 2008. Inferring the favorable adsorption level and the concurrent multi-stage process with the Freundlich constant. *J. Hazard. Mater.* 155, 277–287. <https://doi.org/10.1016/j.jhazmat.2007.11.061>.
- Ukalska-Jaruga, A., Debaena, G., Smreczak, B., 2019. Dissipation and sorption processes of polycyclic aromatic hydrocarbons (PAHs) to organic matter in soils amended by exogenous rich-carbon material. *J. Soils Sediment.* 20, 836–849. <https://doi.org/10.1007/s11368-019-02455-8>.
- Valo, R., Kitunen, V., Salkinoja-Salonen, M., Räisänen, S., 1984. Chlorinated phenols as contaminants of soil and water in the vicinity of two Finnish sawmills. *Chemosphere* 13, 835–844. [https://doi.org/10.1016/0045-6535\(84\)90156-5](https://doi.org/10.1016/0045-6535(84)90156-5).
- Wang, Y.-S., Li, D.-B., Zhang, F., Tong, Z.-H., Yu, H.-Q., 2018. Algal biomass derived biochar anode for efficient extracellular electron uptake from *Shewanella oneidensis* MR-1. *Front. Environ. Sci. Eng.* 12. <https://doi.org/10.1007/s11783-018-1072-5>.
- Wu, S., Fang, G., Wang, Y., Zheng, Y., Wang, C., Zhao, F., Jaisi, D.P., Zhou, D., 2017. Redox-Active Oxygen-Containing Functional Groups in Activated Carbon Facilitate Microbial Reduction of Ferrihydrite. *Environ. Sci. Technol.* 51, 9709–9717. <https://doi.org/10.1021/acs.est.7b01854>.
- Xu, S., Adhikari, D., Huang, R., Zhang, H., Tang, Y., Roden, E., Yang, Y., 2016. Biochar-Facilitated Microbial Reduction of Hematite. *Environ. Sci. Technol.* 50, 2389–2395. <https://doi.org/10.1021/acs.est.5b05517>.
- Xu, X., Huang, H., Zhang, Y., Xu, Z., Cao, X., 2019. Biochar as both electron donor and electron shuttle for the reductive transformation of Cr(VI) during its sorption. *Environ. Pollut.* 244, 423–430. <https://doi.org/10.1016/j.envpol.2018.10.068>.
- Xu, Y., Liu, J., Cai, W., Feng, J., Lu, Z., Wang, H., Franks, A.E., Tang, C., He, Y., Xu, J., 2020. Dynamic processes in conjunction with microbial response to disclose the biochar effect on pentachlorophenol degradation under both aerobic and anaerobic conditions. *J. Hazard. Mater.* 384, 121503. <https://doi.org/10.1016/j.jhazmat.2019.121503>.
- Xu, Y., Yan, Y., Obadamudalige, N.L., Ok, Y.S., Bolan, N., Li, Q., 2019. Redox-Mediated Biochar-Contaminant Interactions in Soil. *Biochar from Biomass and Waste. In: Biochar from Biomass and Waste. Elsevier.*
- Yang, J., Pignatello, J.J., Pan, B., Xing, B., 2017. Degradation of p-Nitrophenol by Lignin and Cellulose Chars: H₂O₂-Mediated Reaction and Direct Reaction with the Char. *Environ. Sci. Technol.* 51, 8972–8980. <https://doi.org/10.1021/acs.est.7b01087>.
- Yu, L., Yuan, Y., Tang, J., Wang, Y., Zhou, S., 2015. Biochar as an electron shuttle for reductive dechlorination of pentachlorophenol by *Geobacter sulfurreducens*. *Sci. Rep.* 5. <https://doi.org/10.1038/srep16221>.
- Yuan, Y., Bolan, N., PrévotEAU, A., Vithanage, M., Biswas, J.K., Ok, Y.S., Wang, H., 2017. Applications of biochar in redox-mediated reactions. *Bioresour. Technol.* 246, 271–281. <https://doi.org/10.1016/j.biortech.2017.06.154>.
- Zhang, C., Zhang, N., Xiao, Z., Li, Z., Zhang, D., 2019. Characterization of biochars derived from different materials and their effects on microbial dechlorination of pentachlorophenol in a consortium. *RSC Adv.* 9, 917–923. <https://doi.org/10.1039/c8ra09410a>.
- Zhang, K., Sun, P., Faye, M.C.A.S., Zhang, Y., 2018. Characterization of biochar derived from rice husks and its potential in chlorobenzene degradation. *Carbon* 130, 730–740. <https://doi.org/10.1016/j.carbon.2018.01.036>.

- Zheng, H., Zhang, C., Liu, B., Liu, G., Zhao, M., Xu, G., Luo, X., Li, F., Xing, B., 2020. Biochar for Water and Soil Remediation: Production, Characterization, and Application. In: *Paradigm for Environmental Chemistry and Toxicology: From Concepts to Insights*. Springer, Singapore. <https://doi.org/10.1007/978-981-13-9447-8>.
- Zhou, G.-W., Yang, X.-R., Marshall, C.W., Li, H., Zheng, B.-X., Yan, Y., Su, J.-Q., Zhu, Y.-G., 2017. Biochar Addition Increases the Rates of Dissimilatory Iron Reduction and Methanogenesis in Ferrihydrite Enrichments. *Front. Microbiol.* 8. <https://doi.org/10.3389/fmicb.2017.00589>.
- Zhu, M., Lv, X., Franks, A.E., Brookes, P.C., Xu, J., He, Y., 2020. Maize straw biochar addition inhibited pentachlorophenol dechlorination by strengthening the predominant soil reduction processes in flooded soil. *J. Hazard. Mater.* 386, 122002. <https://doi.org/10.1016/j.jhazmat.2019.122002>.
- Zhu, M., Zhang, L., Zheng, L., Zhuo, Y., Xu, J., He, Y., 2018. Typical Soil Redox Processes in Pentachlorophenol Polluted Soil Following Biochar Addition. *Front. Microbiol.* 9. <https://doi.org/10.3389/fmicb.2018.00579>.